

Investigation of Cure Kinetics in Epoxy/Multiwalled Carbon Nanotube Nanocomposites

Samuel Brando Susin,¹ Vinicius Pistor,² Sandro Campos Amico,² Luiz Antonio Ferreira Coelho,³ Sergio Henrique Pezzin,³ Ademir José Zattera¹

¹Laboratory of Polymers, Center of Exact Sciences and Technology (CCET), Caxias do Sul University (UCS), Caxias do Sul/RS, Brazil

²Federal University of Rio Grande do Sul (UFRGS), Porto Alegre/RS, Brazil

³Center for Technological Sciences, State University of Santa Catarina (UDESC), Joinville/SC, Brazil

Correspondence to: A. J. Zattera (E-mail: ajzatter@ucs.br)

ABSTRACT: With the increased interest in thermoset resin nanocomposites, it is important to understand the effects of the material on nanoscale characteristics. In this study, a curing reaction of an epoxy resin, which contained 0.25, 0.50, or 1.00 wt % of multiwalled carbon nanotubes (MWCNTs), at different heating rates was monitored by differential scanning calorimetry; cure kinetics were also evaluated to establish a relationship between crosslinking (network formation) and mechanical properties. MWCNT concentrations above 0.25 wt % favored crosslinking formation and decreased the activation energy (E_a) in the curing reaction. Examination of the kinetic mechanism suggests that the MWCNT locally restricted the spatial volume and favored the formation of nodular morphology in the resin, especially for high MWCNT concentrations. The MWCNT exhibited some entanglement in the matrix, which hindered a more pronounced effect on the mechanical properties. © 2013 Wiley Periodicals, Inc. *J. Appl. Polym. Sci.* **2014**, *131*, 39857.

KEYWORDS: kinetics; nanotubes; graphene and fullerenes; thermosets; differential scanning calorimetry; morphology

Received 19 June 2013; accepted 15 August 2013

DOI: 10.1002/app.39857

INTRODUCTION

Among the variety of nanoscale materials examined over the last few years, carbon nanotubes (CNTs) have attracted special interest due to certain characteristics: a large surface area (300–1000 m²/g range), a minimum aspect ratio of 1000, a thermal conductivity *ca.* three times higher than the thermal conductivity of diamond, an electrical conductivity *ca.* 1000 times higher than the electrical conductivity of copper wires, a mechanical strength 100 times higher than the mechanical strength of steel (considering the weight ratio between their mechanical strengths) and a maximum elastic modulus of 1 TPa.^{1,2}

There is significant interest in the use of nanotubes to enhance the properties of epoxy resins. However, certain factors, such as interfacial interaction, inefficient dispersion and alignment of CNTs, can hinder or even prevent this effect, which produces clusters of entanglements. These factors have been considered critical for achieving enhanced properties.^{2–4} Due to the inherent difficulties associated with these factors, researchers have reported distinct values of certain properties, e.g., elastic modulus, using equivalent concentrations of CNTs.^{5–7}

Another theory that may explain these differences is related to the potential effect of CNTs on the curing reaction and the density of crosslinking bonds. Due to steric hindrance, the dispersion of CNTs has been demonstrated to alter the enthalpy of the curing reaction.⁸ The addition of CNTs can reduce the E_a of the reaction through a catalytic effect.⁹ Previous studies^{10,11} and recent studies^{12,13} have examined the inhomogeneous cure of epoxy resins, which results in a microstructure composed of nodular regions with variable crosslinking density.¹¹ Because these fluctuations are independent of the stoichiometry, nodular interfaces are produced independently of the ratio between epoxy and amine groups. These interfaces exhibit an important effect on the modification of physical and mechanical characteristics of the material.

The aim of this study is to investigate the correlation between the cure kinetics and mechanical properties of an epoxy resin containing multiwalled carbon nanotubes (MWCNTs).

EXPERIMENTAL

An epoxy resin based on bisphenol A and epichlorohydrin [Araldite[®] GY 251 (diglycidyl ether of bisphenol A

Table I. Algebraic Expressions for $g(\alpha)$ and $f(\alpha)$ for the Predominantly Used Mechanisms of Solid State Processes

Mechanism	$g(\alpha)$	$f(\alpha)$
A ₂ , Nucleation and growth [Avrami equation (1)]	$[-\ln(1-\alpha)]^{1/2}$	$2(1-\alpha)[- \ln(1-\alpha)]^{1/2}$
A ₃ , Nucleation and growth [Avrami equation (2)]	$[-\ln(1-\alpha)]^{1/3}$	$3(1-\alpha)[- \ln(1-\alpha)]^{2/3}$
A ₄ , Nucleation and growth [Avrami equation (3)]	$[-\ln(1-\alpha)]^{1/4}$	$4(1-\alpha)[- \ln(1-\alpha)]^{3/4}$
R ₁ , Controlled reaction on the surface (motion in one dimension)	α	1
R ₂ , Controlled surface reaction (contraction dimensional)	$[-\ln(1-\alpha)]^{1/2}$	$2(1-\alpha)^{1/2}$
R ₃ , Controlled reaction on the surface (migration volume)	$[-\ln(1-\alpha)]^{1/3}$	$3(1-\alpha)^{2/3}$
D ₁ , Diffusion in one dimension	α^2	$(1/2)\alpha^{-1}$
D ₂ , Diffusion in two dimension (Valensi equation)	$(1-\alpha)\ln(1-\alpha)+\alpha$	$-\ln(1-\alpha)^{-1}$
D ₃ , Diffusion in three dimensions (Jander equation)	$[-\ln(1-\alpha)]^{1/3}{}^2$	$(3/2)[1-(1-\alpha)^{1/3}]^{-1}(1-\alpha)^{2/3}$
D ₄ , Diffusion in three dimensions (Ginstling–Brounshtein equation)	$[1-(2/3)\alpha]-(1-\alpha)^{2/3}$	$(3/2)[1-(1-\alpha)^{1/3}]^{-1}$
F ₁ , Random nucleation with one nucleus of individual particle	$-\ln(1-\alpha)$	$1-\alpha$
F ₂ , Random nucleation with two nuclei of individual particle	$1/(1-\alpha)$	$(1-\alpha)^2$
F ₃ , Random nucleation with three nuclei of individual particle	$1/(1-\alpha)^2$	$(1/2)(1-\alpha)^3$

(DGEBA)] and a triethylenetetramine (TETA; REN HY 956 BR) crosslinking agent, which were both supplied by Huntsman[®], were employed in this study. MWCNTs (Baytubes[®] C150 P) were produced by chemical vapor deposition (CVD) and supplied in agglomerated form by Bayer[®]. According to the manufacturer, the MWCNT (3–15 layers) presented 95% purity degree, with internal and external diameters of 2–6 nm and 5–20 nm, respectively, and a length within the range of 1–10 μm .

Epoxy resin containing 0.25, 0.50, and 1.00 wt % of MWCNT were mixed using Sonics sonication equipment, VCX 750 model, operated at 225 W for 20 min. The DGEBA epoxy resin was prepared based on the equivalents of reactive groups (g/eq). A molar ratio of 1/1 (g/eq) between the epoxy and amine groups was maintained. Curing of the resin was performed at 25°C for 24 h. Subsequently, the samples were post-cured for 24 h at 100°C. A neat epoxy resin (i.e., without MWCNT) was also prepared for comparison.

The samples were prepared by transmission electron microscopy (TEM) using cryoultramicrotomy and were mounted on cryopins. TEM analyses were conducted with a Philips microscope (W503S model) operated at 80 kV with a filter. The tensile strength was measured on Type I specimens (ASTM D638) using a Universal Testing Machine (EMIC DL 3000) operated at 5 mm/min and an extensometer.

The curing process of the epoxy/MWCNT samples was monitored by differential scanning calorimetry (DSC) using a Shimadzu DSC50 apparatus under nitrogen atmosphere (40 mL/min). The curing agent (TETA) was added to the resin; the samples (*ca.* 10 mg) were promptly analyzed by DSC and heated at temperatures in the range of 25–250°C with various heating rates (5, 10, 20, and 40°C/min). The DSC results were applied to estimate the kinetic parameters based in the Flynn–Wall–Ozawa (FWO) [eq. (1)]^{14,15} and Criado [eq. (2)]¹⁶ equations.

$$\log(\beta) = \log\left(\frac{AE_a}{R}\right) - \log(g(\alpha(T))) - 2.315 - 0.4567 \frac{E_a}{RT} \quad (1)$$

$$Z(\alpha) = \frac{d\alpha}{dT} \frac{E_a}{R} e^{\frac{E_a}{RT}} P(\alpha) \quad (2)$$

where α is the conversion rate, T is the absolute temperature, β is the heating rate, R is the gas constant, E_a is the activation energy, A is a pre-exponential factor, $Z(\alpha)$ is the kinetic mechanism, and $P(\alpha)$ is a function that can be solved by a rotational expression.^{16,17}

The FWO method is an isoconversional method that estimates E_a by considering that the reaction mechanism is a function of temperature.^{14,15,17} Thus, using different heating rates, it is possible to determine E_a over the entire α range studied. By establishing E_a , the kinetic mechanism of the reaction can be determined using the Criado method.¹⁶ This method involves overlapping experimental data obtained using eq. (2) with different theoretical curves obtained using eq. (3) and Table I¹⁷ as follows:

$$Z(\alpha) = f(\alpha)g(\alpha) \quad (3)$$

RESULTS AND DISCUSSION

Figure 1 displays the results of the TEM analysis of the nanocomposite samples. MWCNT clusters were distributed within the sonicated polymeric matrix. The ultrasound produces cavitation based on the pulse of mechanic waves and the induced shear promotes the separation of nanotubes as shown in the TEM images. However, tip sonication can promote breaking of the CNT and reduction in length with an expected detrimental effect on mechanical properties.⁸

Table II presents tensile modulus, tensile strength, and strain at break for the samples. These properties show a trend toward higher modulus and strength and a trend toward lower strain for higher MWCNT contents. Although it can be debated that the variations are in the expected range,¹⁸ these effects are

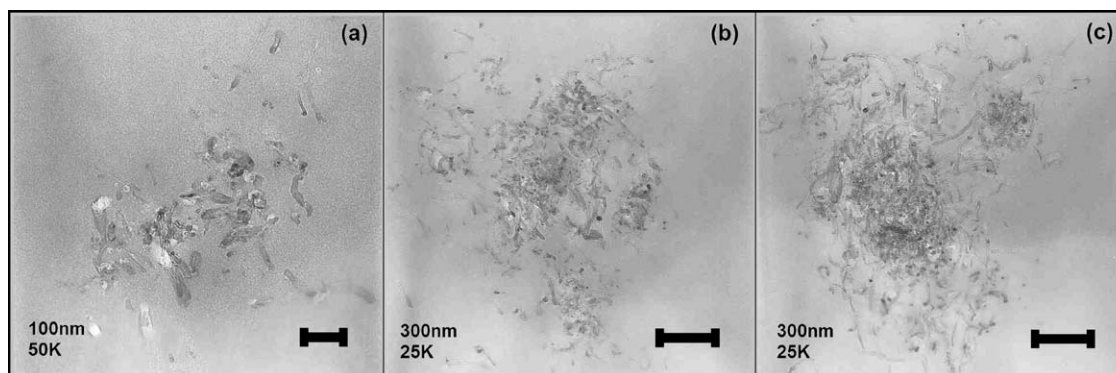


Figure 1. TEM images of the epoxy nanocomposites with 0.25, 0.50, and 1.00 wt % MWCNT ((a)–(c), respectively).

Table II. Tensile Properties of the Samples

Sample	Tensile modulus (GPa)	Tensile strength (MPa)	Strain at break (%)
Epoxy Resin	2.3 ± 0.2	43.5 ± 0.8	4.9 ± 0.6
0.25 wt % MWCNT	2.4 ± 0.1	44.3 ± 2.7	3.1 ± 0.4
0.50 wt % MWCNT	2.7 ± 0.2	48.3 ± 3.3	2.8 ± 0.6
1.00 wt % MWCNT	2.9 ± 0.1	48.2 ± 3.4	2.8 ± 0.7

influenced by two other factors that reduce the aspect ratio of the nanotubes or influence the presence of the CNT on the curing degree of the thermoset resin. This correlation has been previously reported.^{19,20} Additionally, the spatial effect of the particles in the nanometric dimension, especially for very short particles such as nanotubes, can influence curing behavior.

The thermograms of the curing reaction monitored by DSC are displayed in Figure 2. It was used the $\beta = 5^\circ\text{C}/\text{min}$ as a representative thermograms, however, the all heating rates showed the same trend. Resin curing is an exothermic process that can be qualitatively monitored through observations of parameters, such as the generated heat (ΔH), the maximum temperature

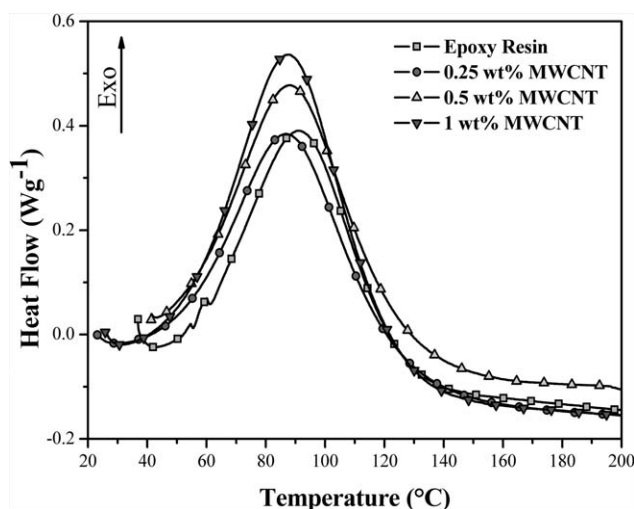


Figure 2. DSC thermograms for the samples obtained at $5^\circ\text{C}/\text{min}$ during the curing process.

achieved during curing (T_{max}), the height of the curve and the variation in temperature (i.e., width) at half-height (T_{HW}). These parameters are shown in Table III.

Compared with the neat epoxy resin, the addition of the MWCNT reduced T_{max} , i.e., the process occurs at lower energy levels. The presence of MWCNTs may increase the probability area of collision between functional groups due to the barrier effect and may also produce high thermal conductivity of the nanotubes. The barrier effect may be attributed to the reduction in volume fluctuation of the reaction, i.e., considering that an equivalent quantity of polymeric chains exists per unit of area in both systems, the addition of the nanotubes for the pure epoxy resin and the nanocomposites tends to reduce the volume of voids in the system; therefore, it decreases the average distances that the reactants are required to travel to form chemical bonds in the curing process.

Although the ΔT_{HW} did not change, the height of the curves increased with MWCNT content. Both parameters are associated with reaction homogeneity, which may depend on the concentration at the reaction sites. The increase in height of the curves corresponds to the reduction in volume fluctuations of the reaction, i.e., the reaction between the functional groups occurs at a smaller temperature range. The ΔH values corroborate the homogeneity associated with the addition of MWCNT to the epoxy resin. The increase in reaction heat and the lower temperatures suggest that the reaction for the nanocomposites occurs more favorably and homogeneously.

DSC analyses were performed at different heating rates to evaluate the cure kinetics. Figure 3 displays the results obtained for the neat epoxy resin cured at $\beta = 5, 10, 15,$ and $20^\circ\text{C}/\text{min}$. The increase in β shifts the curing process to higher temperatures,

Table III. Parameters Obtained by DSC Analysis

Sample	T_{\max} (°C)	ΔT_{HW} (°C)	Height (W/g)	ΔH (J/g)
Epoxy Resin	90.9	40.1	0.451	251.3
0.25 wt % MWCNT	86.9	41.8	0.456	272.1
0.50 wt % MWCNT	87.7	40.8	0.492	286.2
1.00 wt % MWCNT	87.5	40.8	0.606	351.5

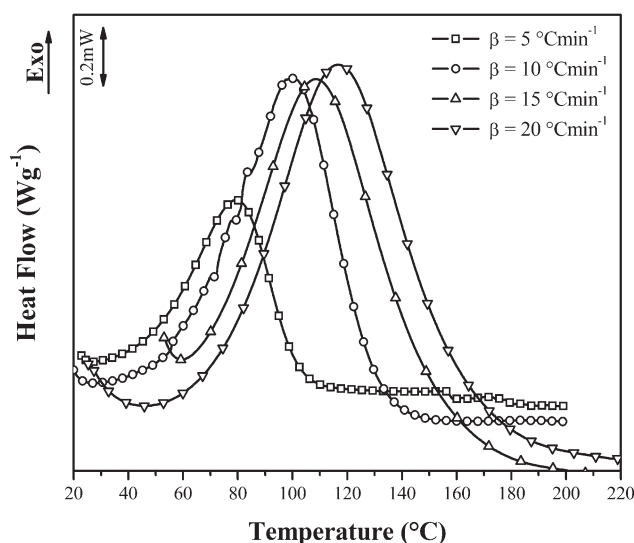
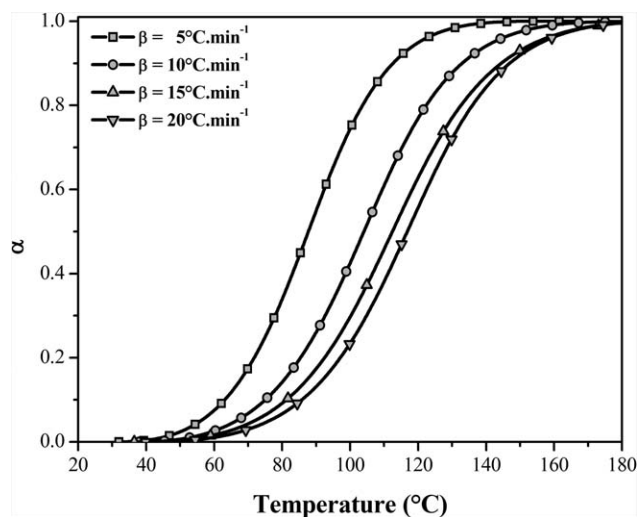
with a well-defined increase in ΔH of the reaction (e.g., for the epoxy resin, the values of ΔH were 251.3, 314.5, 318.8, and 327.2 J/g for $\beta = 5, 10, 15,$ and $20^\circ\text{C}/\text{min}$, respectively). This result is expected when more heat is provided during short intervals under non-isothermal conditions. The use of shifted curves as a function of temperature, which is illustrated in Figure 4, enables the determination of the conversion values ($\alpha(T)$) using eq (4).

$$\alpha(T) = \frac{\int_{T_0}^T dH/dT dT}{\int_{T_0}^{T_\infty} dH/dT dT} \quad (4)$$

where dH is the heat of the reaction, T_0 is the temperature at the initial conversion, T is the temperature at each arbitrary time, and T_∞ is the final temperature of the conversion curve.

Figure 5 shows the results of the analysis using the FWO method, which was applied to the epoxy resin (all samples exhibited similar behavior). The linear fitting of the $\log \beta$ versus $1/T$ data for all samples yielded coefficients of determination (R^2) that was near unity (0.9899–0.1000) with a confidence level of 95%.

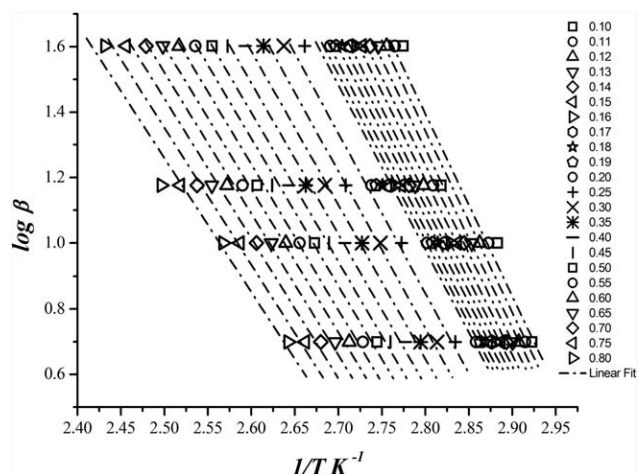
Figure 6 shows the E_a values in the range of 0.1–0.8 as a function of α . The E_a values obtained for the epoxy resin were ≈ 100 kJ/mol for $\alpha = 0.1$ and decreased with α (≈ 75 kJ/mol for

**Figure 3.** Thermogram of the curing reaction of neat epoxy resin obtained at various β .**Figure 4.** Conversion curves obtained by the integration area of the thermograms.

$\alpha = 0.8$). The decrease in E_a is due to the consumption of reactive groups present in the reaction. The addition of 0.25 wt % of MWCNT did not alter the E_a because this small amount was insufficient for achieving homogeneous distribution within the reaction medium.

The samples containing 0.50 and 1.00 wt % of MWCNT exhibited a significant reduction in E_a throughout the reaction. This reduction is consistent with the catalytic effect suggested in the literature⁹: being favored by the high thermal conductivity of the nanotubes. In terms of energy, a reduction in E_a indicates that the spatial growth of crosslinking bonds is facilitated by the narrowing of gaps through which the molecules must travel to produce chemical bonds. This occurrence may not yield modified reaction times because the reaction velocity rate is only dependent on the reactivity of the functional groups.

Figure 7 presents the chemical mechanisms of the reaction using the Criado method.¹⁹ This method involves overlapping experimental data with the master curves that represent different

**Figure 5.** FWO plot for the determination of the E_a in the epoxy curing process.

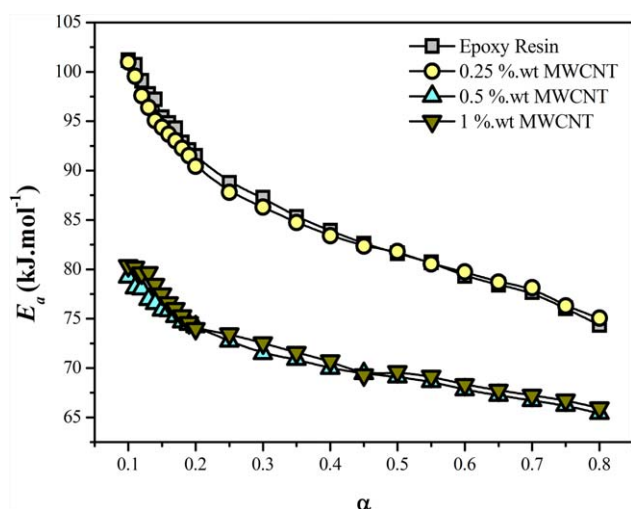


Figure 6. E_a values obtained by the FWO method for all samples. [Color figure can be viewed in the online issue, which is available at wileyonlinelibrary.com.]

mechanisms, as illustrated in Table I. The master curves are classified as nucleation and growth (A_n), a reaction controlled by the surface (R_n), a diffusion reaction (D_n) and a deceleratory reaction through individual nucleus formation (F_n ; Table I), in which the subscript n represents the reaction order.

For the neat epoxy resin [Figure 7(a)], the mechanism appears to follow two stages. In the first stage, for a maximum α of 0.4, the F_1 mechanism was prevalent, i.e., the deceleratory mechanism that occurs due to the nuclei formation characteristics of the polyaddition process of the functional groups (related to the nodular formation of the epoxy resin¹¹). Because this process is dependent on the consumption of reactants, random nuclei formation is expected to occur. With progress of the reaction, the experimental data approaches the F_3 mechanism for $\alpha > 0.4$. This change demonstrates that more reticulated nuclei are produced for higher conversions, which progressively increases their size due to the consumption of reactants. This change in reaction rate at higher conversion values is expected for systems that react to the polyaddition of functional groups. In addition, the epoxy resin curing system is considered kinetically inhomogeneous due to the formation of nodular regions with variation in the crosslinking density during the reaction.^{10–13} In the first stage of the crosslinking, microgels are formed and as the reaction proceeds, the molecular weight tends to increase, causing a reduction in diffusivity of the molecules in the reaction environment.¹¹ This process generally progresses until the total consumption of reactants is completed. At a particular point in the reaction, growth in the crosslinked network is hindered and the diffusion of non-reacted molecules is restricted. At this point, an interface between microgels is evident and the nodular formation changes the velocity of the reaction. Although a constant rate of consumption of reactants is initially maintained in

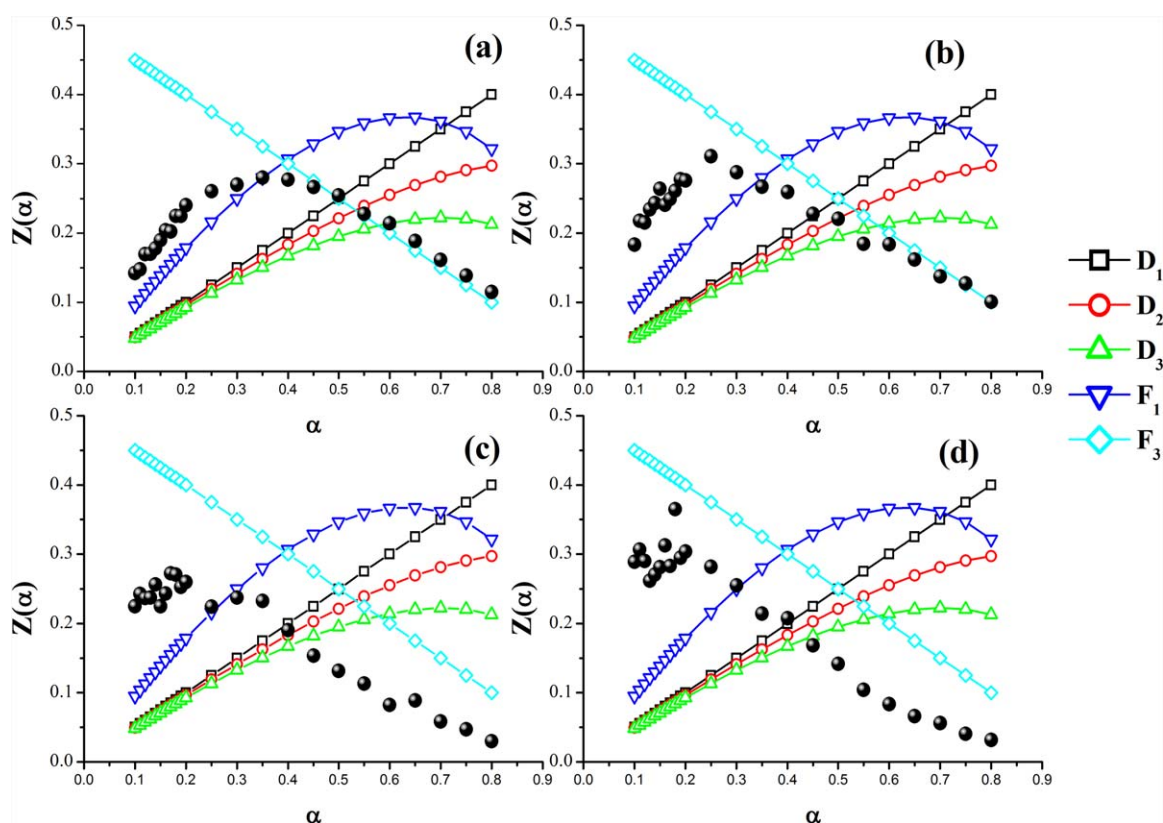


Figure 7. Cure kinetic mechanism obtained by the Criado method for (a) Neat epoxy resin, (b) 0.25 wt % MWCNT, (c) 0.50 wt % MWCNT, and (d) 1.00 wt % MWCNT. [Color figure can be viewed in the online issue, which is available at wileyonlinelibrary.com.]

the curing process, the probability of nodule growth, which propagates the reaction, is equivalent in each space of the reaction volume. However, with the addition of MWCNT, the epoxy resin approaches the F_3 mechanism along the entire conversion range shown. This effect was more pronounced for higher MWCNT contents. These results suggest that the presence of the MWCNT promotes the crosslinking reaction due to greater nuclei reticulation. This finding may provide an overall explanation for the lower E_a values, the higher intensity peaks and the reduction in reaction temperatures monitored by DSC.

CONCLUSIONS

Multiwalled carbon nanotubes (MWCNTs) were dispersed in epoxy resin using ultrasound. The curing reaction was monitored by DSC analysis to evaluate its relationship with the mechanical properties. The MWCNTs were found to increase the ΔH of the reaction and shift the reaction temperature to lower values due to the presence of the carbon nanotubes. However, the E_a obtained by the FWO method indicated that the reaction is facilitated by the addition of 0.50 or 1.00 wt % of MWCNT. This reduction of E_a is caused by the reduction in spatial volume, which promotes collision between reactive groups. The kinetic Criado mechanism corroborates this finding and demonstrates that the presence of nanotubes produces a more homogenous reaction that decelerates nucleation in three dimensions. This effect is expected to be more pronounced if a higher amount of CNT is incorporated in resin employed for advanced thermoset nanocomposite applications.

ACKNOWLEDGMENTS

The authors gratefully acknowledge UCS, CAPES, CNPq, and FAPERGS for their scholarships and financial support.

REFERENCES

1. Ijima, S. *Nature* **1991**, 367, 185.
2. Xie, X. L.; Maia, Y. W.; Hou, Z. X. *P. Mater. Sci. Eng.* **2005**, 49, 89.
3. Chen, W.; Auad, M. L.; William, R. J. J.; Nutt, S. R. *Eur. Polym. J.* **2006**, 42, 2765.
4. Battisti, A.; Skordos, A. A.; Partridge, I. K. *Compos. Sci. Technol.* **2009**, 69, 1516.
5. Hernández-Pérez, A. H.; Avilés, F.; Pat, A. M.; González, A. V.; Franco, P. J. H.; Pérez, P. B. *Compos. Sci. Technol.* **2008**, 68, 1422.
6. Allaoui, A.; Bai, S.; Cheng, H. M.; Bai, J. B. *Compos. Sci. Technol.* **2002**, 62, 1993.
7. Lau, K.; Lu, M.; Lam, C.; Cheung, H.; Sheng, F.; Li, H. *Compos. Sci. Technol.* **2005**, 65, 719.
8. Kim, S. H.; Lee, W. I.; Park, J. M. *Carbon* **2009**, 47, 2699.
9. Zhou, T.; Wang, X.; Liu, X.; Xiang, D. *Carbon* **2009**, 47, 1112.
10. Vanlandingham, M. R.; Eduljee, R. F.; Gillespie Jr, J. W. *J. Appl. Polym. Sci.* **1999**, 71, 699.
11. Pascault, H. S.; Verdu, J.; Williams, R. J. J. *Thermosetting Polymers*; Marcel Dekker: New York, **2002**.
12. Pistor, V.; Barbosa, L. G.; Soares, B. G.; Mauler, R. S. *Polymer* **2012**, 53, 5798.
13. Pistor, V.; Soares, B. G.; Mauler, R. S. *Polymer* **2013**, 54, 2292.
14. Flynn, J. H.; Wall, L. A. *J. Res. Natl Bureau Stand.* **1996**, 70, 487.
15. Ozawa, T. A. *Bull. Chem. Soc. Jpn.* **1966**, 39, 2071.
16. Criado, J. M.; Malek, J.; Ortega, A. *Thermochim. Acta* **1989**, 147, 377.
17. Poletto, M.; Pistor, V.; Zeni, M.; Zattera, A. *J. Polym. Degrad. Stab.* **2011**, 96, 679.
18. Pizzutto, C. E.; Suave, J.; Bertholdi, J.; Pezzin, S. H.; Coelho, L. A. F.; Amico, S. C. *Mater. Res. Ibero-American J. Mater.* **2011**, 14, 256.
19. Abdalla, M.; Dean, D.; Robinson, P.; Nyairo, E. *Polymer* **2008**, 49, 3310.
20. Abdalla, M.; Dean, D.; Adibemped, D.; Nyairo, E.; Robinson, P.; Thompson, G. *Polymer* **2007**, 48, 5662.